Photoluminescence of nc-Si/SiN Superlattices Embedded in Optical Microcavities*

Chen San, Qian Bo, Chen Kunji†, Cen Zhanhong, Liu Yansong, Han Peigao, Ma Zhongyuan, Xu Jun, Li Wei, and Huang Xinfan

(*National Laboratory of Solid State Microstructures, Department of Physics, Nanjing University, Nanjing* 210093, *China*)

Abstract: We fabricate a-Si/a-SiN$_z$ superlattices and a one-dimensional amorphous silicon nitride photonic crystal microcavity by plasma enhancement chemical vapor deposition (PECVD). To improve the light-emitting efficiency of the nc-Si/a-SiN$_z$ superlattices, which are made from a-Si/a-SiN$_z$ superlattices by laser annealing, an nc-Si quantum dot array is inserted into the photonic crystal microcavity. Raman spectroscopy and transmission electron microscopy analysis show that nc-Si with a size of 4nm, which is close to the designed thickness of the a-Si sublayers, is formed in the a-Si sublayers. Owing to microcavity effects, the PL peak of the nc-Si/a-SiN$_z$ superlattices embedded in the microcavity is strongly narrowed, and the intensity of the PL is enhanced by two orders of magnitude with respect to the emission of $\lambda/2$-thick nc-Si/a-SiN$_z$ superlattices. Light emission at a cavity-resonant frequency from the nc-Si/a-SiN$_z$ superlattices is enhanced while other frequencies are forbidden. This leads to the narrowing of the PL spectrum and enhancement of the intensity.

Key words: microcavity; photonic crystal; photoluminescence
PACC: 7855
CLC number: O472$^+$.3　　**Document code**: A　　**Article ID**: 0253-4177(2006)S0-0025-04

1 Introduction

Integrating optical functionality into silicon microelectronic chips is one of the most challenging problems of material research. For a long time, silicon has been considered unsuitable for optoelectronic applications because its indirect bandgap makes it an inefficient emitter of light. In the recent decades, research has been devoted to different approaches for overcoming the physical inability of silicon to act as an efficient emitter at room temperature. The intense visible light emission from porous silicon[1] motivated the synthesis of low-dimensional Si systems and the investigation of their light-emitting properties. Porous silicon formed by electrochemical etching can emit light that covers the whole visible light range, from the near infrared to the ultraviolet, by adjusting the porosity. Due to chemical and mechanical unstability and difficulty in precisely controlling the sizes of nanocrystals, other low-dimensional Si systems have been used to improve light-emitting efficiency. Pavesi *et al*.[2] fabricated silicon nanocrystals that were embedded in a SiO_2 matrix through negative ion implantation into ultra-pure quartz substrates or into a thermally grown SiO_2 layer on Si substrates and a high-temperature thermal annealing process. Intense photoluminescence (PL) with a peak at about 800nm was observed, and an optical gain at 100cm^{-1} was also obtained with the variable strip length method, with the results that are comparable to those found in Ⅲ-Ⅴ semiconductor quantum dots. However, broad size distribution like that of nanocrystals in porous silicon is still a key issue that hinders the further improvement of light-emitting efficiency. Si/wide bandgap insulator, especially, Si/SiO_2 superlattices, have received much attention. Lockwood *et al*.[3] studied light emission from SiO_2/Si superlattices and observed the quantum confinement effect from PL.

* Project supported by the National Natural Science Foundation of China (Nos. 10174035, 90301009, 10374049), the Natural Science Foundation of Jiangsu Province (No. BK2002407), and the State Key Development Program for Basic Research of China (No. 2001CB610503)

† Corresponding author. Email: kjchen@netra.nju.edu.cn

Received 16 November 2005

For low-dimensional silicon systems, the PL is size-dependent. A quantum confinement model was proposed to interpret the mechanism responsible for the PL spectrum of nanocrystal Si. In Ref. [2], the authors gave a three-level model in which the Si/SiO_2 interface states play an important role in the radiative recombination of carriers and optical gain. Based on the self-consistent tight-binding method[4], Wolkin *et al*.[5] calculated electronic states in Si nanocrystals as a function of cluster and surface passivation, and they identified two competing recombination mechanisms: the quantum confinement of excitons and recombination through interface states. Other mechanisms[6,7] have also been proposed. To date, the mechanism of low-dimensional silicon-based systems is still debatable, but to improve the light-emitting efficiency of Si, a defect-free, atomically flat, compositionally abrupt Si/SiO_2 interface, regular shape of nano-particles, and uniform size are absolutely essential.

It has recently been discovered that nc-Si can exhibit optical gain[2,8]. However, there are still some problems that currently strongly limit the application of nc-Si for the manufacturing of optoelectronic devices, namely, the absence of spectral and directionality, low efficiency of light emission, and exact control of the light-emitting peak. In this work, we report the photoluminescence of nc-Si/a-SiN_z superlattices formed by laser annealing of a-Si thin films, which are grown by plasma enhancement chemical vapor deposition (PECVD). In order to improve the light emission from nc-Si/SiN_z superlattices, this light-emitting medium as a defect was inserted into a one-dimensional photonic crystal, which forms a one-dimensional photonic crystal microcavity. Photon states in free space are redistributed because of modulation of this kind of composite structure, and as a result, radiative transition in nc-Si/a-SiN_z superlattices are be modulated. A JY T64000 with the 488 line of an Ar^+ laser is used for Raman and PL spectra measurements. Cross-section TEM analysis is also presented.

2 Experiment

The stacking layers for the present one-dimensional photonic crystal microcavity structures were grown on Corning 7059 glass substrates at 250℃ by PECVD. The decomposition of silane and silane/ammonia was performed at 37.33Pa with an RF power of 30W. In the deposition chamber, two different silane/ammonia flux ratios are periodically alternated for the deposition of distributed Bragg reflectors (DBRs) of 6 quarter-wave stacks of a-SiN_x/a-SiN_y with sublayer thicknesses 65nm/97nm and refractive indices 2.8/1.86. Then 11.5-period a-Si/a-SiN_z superlattices with both sides capped by a 20nm a-SiN_z layer, which constitutes the $\lambda/2$ ($\lambda = 725$) cavity, were deposited on the bottom DBRs. The thickness of the sublayers is 4nm for a-Si and 6nm for a-SiN_z. After finishing the deposition of the superlattices, growth was interrupted for the crystallization process for the a-Si/a-SiN_z superlattices by a KrF pulse excimer laser with a pulse duration of 30ns. Finally, the top DBRs, like the bottom ones, were deposited on nc-Si/a-SiN_z superlattices after laser annealing.

The crystallization of the annealed samples was verified by Raman spectroscopy with the backscattering geometry using an Ar^+ laser. The annealed samples were examined by cross-section transmission electron microscopy (TEM); the PL was measured at room temperature using 488nm Ar^+ laser as the excition source.

3 Results and discussion

Figure 1 shows the Raman spectra of the as-deposited sample and the sample annealed with the laser. The Raman spectrum of the as-deposited sample has only one broad band located around $475cm^{-1}$, due to scattering by TO photons of the a-Si sublayers. However, after annealing with the laser, a sharp peak at $517cm^{-1}$ ascribed to the TO model of the nc-Si with a shoulder corresponding to a-Si, emerges in the spectrum, which indicates that nc-Si has formed in the sample. According to the Raman spectrum, the size of the nc-Si in the sample can be estimated to be 4nm, which is close to the designed thickness (4nm) of the a-Si sublayer.

Figure 2 is a cross-section TEM micrograph of the annealed sample. We can see that nc-Si is formed within initial sublayers, which is confirmed by the Raman spectrum. The interfaces be-

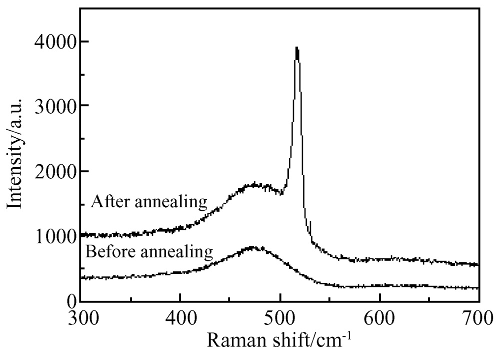

Fig. 1 Raman spectra of as-deposited a-Si/a-SiN_z superlattice samples before and after laser annealing

tween a-Si and a-SiN_z are still flat and abrupt after laser annealing, and in addition, the a-SiN_z sublayers do not change significantly.

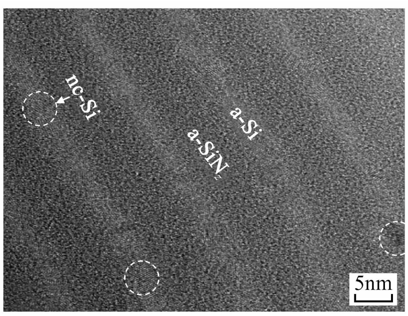

Fig. 2 Cross-section TEM micrograph of a-Si/a-SiN_z superlattices annealed with KrF pulse excimer laser

In order to clarify the microcavity effects on the luminescence of the nc-Si/a-SiN_z superlattices, the PL of the nc-Si/a-SiN_z superlattices are measured under the same conditions as the one from the microcavity. Figure 3 presents the photoluminescence spectra of the nc-Si/a-SiN_z superlattices and the nc-Si/a-SiN_z superlattices embedded

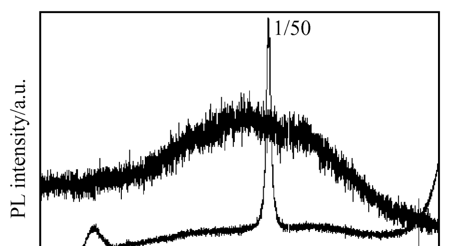

Fig. 3 PL spectrum of the $\lambda/2$-thick nc-Si/a-SiN_z superlattices (with obvious noise) and 1/50 × PL spectrum of the $\lambda/2$ nc-Si/a-SiN_z superlattice microcavity

in the one-dimensional photonic crystal microcavity. The PL spectrum with obvious noise is from the nc-Si/a-SiN_z superlattices, and it has a broad light-emitting band. There are two peaks that we can easily distinguish: the intensive one is located at about 700nm, and the weak one is at 550nm. We roughly estimate the linewith of the peak at 700nm to be more than 150nm. The small signal-to-noise ratio shows that the PL intensity is very weak. For the PL from the nc-Si/a-SiN_z superlattices embedded in the microcavity, we can observe a very sharp and narrow peak at 725nm. This is the cavity resonant peak, with linewidth $\Delta\lambda$ = 5nm. At the two sides, there are two peaks located at the sides of the bandgap of photonic crystal. Because of the high photon state density at the two sides, the luminescence is enhanced, but bigger absorption at shorter wavelengths makes the intensity of the peak at longer wavelengths stronger than that at shorter wavelengths. At the two sides of the cavity resonant peak, the spectrum is relatively flat and is located in the bandgap of the photonic crystal. This shows that the selection of mode is achieved in our samples. Comparing the two PL spectra in Fig. 3, we can see that the wide emission band is strongly narrowed to 5nm, the selected light emission is resonantly enhanced by two orders of magnitude with respect to the emission of $\lambda/2$ thick nc-Si/a-SiN_z superlattices, and other light emission is effectively prohibited. All these phenomena can be interpreted with photonic crystal energy band theory and microcavity effects. In the photon bandgap, the photon state density is very low. When the intrinsic photonic crystal is doped by a defect, a defect state is introduced into the bandgap and is localized in the defect. This defect state (cavity resonant state) has a very high density. According to Fermi's Golden rule, the radiative transition at this cavity resonant frequency is enhanced, and other non-resonant transitions with frequency within the bandgap are prohibited. This is known as the microcavity effect. Therefore light emission at the cavity-resonance frequency from the nc-Si/a-SiN_z superlattices is enhanced, and other frequencies are forbidden. The radiative transition channel at the resonant frequency is the only one, leading to the narrowing of the PL spectrum and enhancement of the intensity.

4 Conclusion

In summary, we fabricated a-Si/a-SiN$_z$ superlattices and an amorphous silicon nitride photonic crystal microcavity. In order to improve the efficiency of the nc-Si/a-SiN$_z$ superlattices formed from a-Si/a-SiN$_z$ superlattices by laser annealing, they were inserted into a photonic crystal microcavity. Owing to microcavity effects, spectral purity and intensity enhancement were obtained. For improving the light emission from Si-based materials, photonic crystal microcavities show promise.

References

[1] Canham L T. Silicon quantum wire array fabrication by electrochemical and chemical dissolution of wafers. Appl Phys Lett, 1990, 57(10): 1045

[2] Pavesi L, Negro L D, Mazzoleni C, et al. Optical gain in silicon nanocrystals. Nature, 2000, 408(6811): 440

[3] Lu Z H, Lockwood D J, Baribeau J M. Quantum confinement and light emission in SiO_2/Si superlattices. Nature, 1995, 378(6554): 258

[4] Lannoo M, Bourgoin J. In: Cardona M. Semiconductor Ⅰ: point defects. New York: Springer-Verlag, 1981

[5] Wolkin M V, Jorne J, Fauchet P M, et al. Electronic states and luminescence in porous silicon quantum dots: the role of oxygen. Phys Rev Lett, 1999, 82(1): 197

[6] Prokes S M. Light emission in thermally oxidized porous silicon: evidence for oxide-related luminescence. Appl Phys Lett, 1993, 62(25): 3244

[7] Brandt M S, Fuchs H D, Stutzmann M, et al. The origin of visible luminescence from 'porous silicon': a new interpretation. Solid State Commun, 1992, 81: 307

[8] Khriachtchev L, Räsänen M, Novikov S, et al. Optical gain in Si/SiO_2 lattice: experimental evidence with nanosecond pulses. Appl Phys Lett, 2001, 79(9): 1249

微腔中 nc-Si/SiN 超晶格的光致发光*

陈 三　钱 波　陈坤基†　岑展鸿　刘艳松　韩培高　马忠元　徐 骏　李 伟　黄信凡

(南京大学物理系 固体微结构国家实验室，南京 210093)

摘要：研究了一维光子晶体微腔结构对 nc-Si/a-SiN$_z$ 超晶格发射的调制.一维光子晶体微腔采用两种具有不同折射率的非化学组分非晶氮化硅的周期调制结构，腔中嵌入采用激光晶化方法制备的硅量子点阵列，从 Raman 谱和透射电子显微镜分析得到其尺寸约为 3～4nm.从光致发光谱上观察到明显的选模作用、明显变窄的发光峰以及约两个量级的发光强度的增强.微腔对硅量子点阵列发光的调制主要表现在两个方面：共振模式的增强和非共振模式的抑制.硅量子点中位于腔共振模式的辐射跃迁被增强，非共振模式的辐射跃迁被抑制，因此位于腔共振频率处的跃迁通道成为硅量子点中唯一的辐射跃迁通道，导致光致发光谱的窄化和强度的增强.因此，在提高硅材料发光效率方面，光子晶体微腔具有非常大的应用前景.

关键词：微腔；光子晶体；光致发光

PACC：7855

中图分类号：O472$^+$.3　　**文献标识码**：A　　**文章编号**：0253-4177(2006)S0-0025-04

* 国家自然科学基金(批准号：10174035，90301009，10374049)，江苏省自然科学基金(批准号：BK2002407)及国家重点基础研究发展规划(批准号：2001CB610503)资助项目

† 通信作者. Email：kjchen@netra.nju.edu.cn

2005-11-16 收到